

# Statics of non uniform Josephson junction parallel arrays: model vs. experiment

F. Boussaha,<sup>1</sup> J.G. Caputo,<sup>2</sup> L. Loukitch,<sup>2</sup> and M. Salez<sup>1</sup>

<sup>1</sup>LERMA, Observatoire de Paris, 77 avenue Denfert-Rochereau, 75014 Paris, France

<sup>2</sup>Laboratoire de Mathématiques, INSA de Rouen B.P. 8, 76131 Mont-Saint-Aignan cedex, France

(Dated: January 13, 2022; version 3.14)

We study experimentally and numerically the zero-voltage supercurrent vs. magnetic field of non-uniform arrays of Josephson junctions parallel-connected by a superconducting stripline. The measured curves are complex, unique and in excellent agreement with numerical simulations using a specially developed model. Using this, we can optimize the arrays to have any desired interference pattern. Such new devices could find applications in magnetometry, quasiparticle mixers and detectors, flux oscillators and superconducting electronics.

PACS numbers: 74.81.Fa, 85.25.Dq

Josephson transmission lines have been experimentally and numerically investigated for their unique properties deriving from the Josephson non-linearity<sup>1,2,3</sup>. Such systems include the "long" Josephson junction (LJJ) and the parallel array of "small" superconducting tunnel junctions connected by a superconducting transmission line, called discrete Josephson transmission line (DJTL)<sup>4,5,6,7</sup>. "Small" vs. "long" qualifies the junction size relative to the Josephson length<sup>2</sup>

$$\lambda_J = \frac{\Phi_0}{2e d J_c} ; \quad (1)$$

where  $\Phi_0 = \hbar/2e$  is the reduced magnetic flux quantum,  $J_c$  is the critical current density and  $d$  is the magnetic thickness<sup>26</sup> between the junction electrodes. A DJTL can also be viewed as a parallel array of  $N-1$  SQUID loops<sup>27,6,7</sup>. For magnetometry, such circuits have been considered recently because they are more sensitive than SQUIDs, the response of their total zero-voltage supercurrent  $I_{max}$  to a magnetic field  $H$  contains much narrower bumps.  $I_{max}(H)$  is then analog to the diffraction pattern of  $N$ -slit optical gratings. Recently non-uniform junction distributions have been considered to synthesize an  $I_{max}(H)$  curve with a single narrow peak at  $H = 0$ , allowing an absolute magnetic zero reference as well as a higher sensitivity<sup>10</sup>. For DJTLs where the Josephson coupling is spatially discontinuous and exists only in the junctions, the difference  $\phi(x;t)$  between the superconducting phases of the top and bottom electrodes obeys an inhomogeneous sine-Gordon equation<sup>20</sup>. When the phases vary little from one junction to another, static and dynamic vortices, i.e. 2 kinks of  $\phi$  can occur in DJTLs. In practice, arrays of small junctions are more flexible than long junctions. They allow better impedance matching, their quasi-particle and surface dampings can be adjusted separately and as we will see here their interference patterns can be designed to suit specific needs. For microwave detection, small junctions have been successfully used to make quantum-noise limited SIS heterodyne mixers and detectors from 100 GHz to 1000 GHz, primarily for radioastronomy<sup>10,11</sup>. These devices use photo-assisted quasiparticle tunneling (the damping term in the sine-Gordon equation). Recently

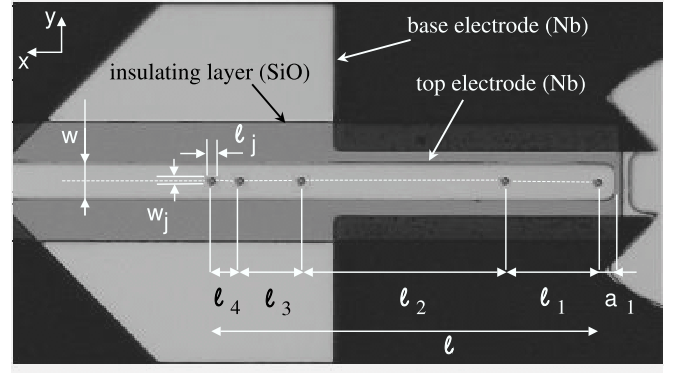


FIG. 1: Photograph of circuit "A" (see Table 1). The 1 m<sup>2</sup> junctions are made out of a Nb-Al-AlOx-Nb trilayer, patterned using a self-aligned process, where the upper Nb layer is removed by RIE around the junction mesas and replaced by SiO<sub>2</sub>. A Nb counter-electrode is then sputtered to contact junctions and make the Nb-SiO<sub>2</sub>-Nb rf tuning microstrip circuit. This one, designed for broadband submillimeter-wave SIS mixing, is also a non-uniform DJTL or SQUID.

SIS mixer designs have mingled with DJTLs<sup>12,24</sup>. In particular, it was demonstrated that a uniform DJTL circumvents the fundamental bandwidth limitation of resistive mixers<sup>13</sup>. We extended this concept to non-uniform arrays with various junction sizes and spacings, to optimize the impedance  $Z(f)$  over virtually any desired submillimeter-wave band (below the superconductor's gap frequency). Such junction arrays behave as multipole bandpass filters<sup>13</sup>. They have also been recently proposed as submillimetric direct detectors. In these applications, the Josephson effect brings excess noise and instabilities. Therefore in practice, one quenches  $I_{max}$  by applying in the plane of the oxide layer a magnetic field corresponding to  $\phi = n\Phi_0$ , where usually  $n = 1$  or  $2$ . Yet the Josephson response to  $H$  of complex, non-uniform DJTLs is not straightforward, due to unknown flux internal distributions, possible phase slippage, ac modes. This initiated our study of Josephson phenomena in SIS-array mixers. This Letter focuses on the static behavior.

The non-uniform SIS-array mixers investigated (see

Table 1 and Fig. 1) consist of  $N = 5$  Nb-AlO<sub>x</sub>-Nb junctions embedded in a Nb-SiO<sub>2</sub>-Nb stripline of width  $w = 5.7 \mu\text{m}$ <sup>14</sup>. The array length is  $l = 80.86 \mu\text{m}$ . Junctions have equal width and length ( $w_j = l_j = 1 \mu\text{m}$ ) and their spacings were optimized so that  $Z(f) \approx 40$  over  $400 - 600 \text{ GHz}$ , for best rf coupling in that range<sup>25</sup>. We successfully applied that design approach to SIS mixers for a spaceborne instrument<sup>12</sup>. The devices were made with a self-aligned, Selective Niobium Etch Process (SNEP) using optical lithography on fused quartz. Critical current densities  $J_c$  range from 5 to  $13 \text{ kA cm}^{-2}$ , junctions have  $V_g = 2.85 \text{ mV}$  and subgap-to-normal resistance ratios of 15–20. The Swihart velocity was measured in LJJJs located on the same wafer, to derive the specific junction capacitance for each batch.  $C_s = 77$  (resp. 81)  $\text{fF } \mu\text{m}^{-2}$  for  $J_c = 5$  (resp. 10)  $\text{kA cm}^{-2}$  are close to the assumed value  $80 \text{ fF } \mu\text{m}^{-2}$ . With a  $250 \text{ nm}$  SiO<sub>2</sub> layer, the Swihart velocity  $c$  in the arrays is  $0.14c$ . In the microwave problem, junctions are point-like and arrays are 1D, since  $l_j < w \ll \lambda = c/f$  over the whole band. The "small junction" approximation is justified because  $l_j < \lambda_j = 5 \text{ m}$ . In a DJTL the size of junctions at rest is defined by the discreteness parameter<sup>7</sup>  $\lambda_j = a$  where  $a$  is the junction spacing.  $\lambda_j > 1$  implies that the flux permeates the array over several cells and that vortices may move freely. For  $\lambda_j < 1$ , vortices must overcome an energy barrier to move from each cell to its neighbor. In our case, there is no periodicity so our discreteness parameter is  $\lambda_j = l_{av}$  where  $l_{av} = l/(N-1)$  is the average distance between junctions. The design and performance of these non-uniform array mixers are detailed elsewhere<sup>13</sup>.

Table 1. Non-uniform DJTL geometry  
(Dimensions of the junctions in  $\mu\text{m}$ ,  $w_j = l_j = 1$ ).

Device	N	w	$a_1$	$l_1$	$l_2$	$l_3$	$l_4$
A	5	5	2	20	42	12	6
B	5	7	2	18	44	11	7
F	2	5	2	12			

We model the device shown in Fig. 1. The phase difference between the top and bottom superconducting layers satisfies in the static regime the following semilinear elliptic partial differential equation<sup>20</sup>

$$\nabla^2 \psi + \frac{g(x;y)}{2} \sin \psi = 0; \quad (2)$$

where  $g(x;y)$  is 1 in the Josephson junctions and 0 outside and we assume the same magnetic thickness  $d$  in all the device. This formulation guarantees the continuity of the normal gradient of  $\psi$ , the electrical current on the junction interface.

The boundary conditions representing an external current input  $I$  and an magnetic field  $H$  applied along  $y$  are

$$\begin{aligned} \psi|_{y=0} &= 0, \quad \frac{I}{2l} d = 0 = I = (2l); \\ \psi|_{x=0} &= H, \quad 0 = \frac{I}{2w} d = 0 = H = (l) \frac{I}{2w}; \end{aligned}$$

where 0 = 1 gives the type of current feed. When  $\psi = 1$  the current is only applied to the long boundaries  $y = 0; w$  (overlap feed) while  $\psi = 0$  corresponds to the

inline feed. The quantities  $H$  and  $I$  are respectively the normalized magnetic field and current.

We consider long and narrow strips containing a few small junctions of area  $l_j \times w_j$  placed on the line  $y = w/2$  and centered on  $x = a_j$ ,  $j = 1; n$ . For narrow strips  $w < \lambda$ , only the first Fourier's mode needs to be taken into account<sup>18</sup>, then we write  $\psi$  as

$$\psi(x;y) = \Gamma(y = w/2)^2 = (lw) + \psi(x).$$

The first term of the equation takes care of the boundary conditions. Thus, we obtain the following equation for  $\psi$ :

$$\nabla^2 \psi + G(x) [w_j = (w/2)] \sin \psi = 0;$$

where  $\Gamma = w$ . We restrict ourselves to small junctions and we consider that the phase does not vary in the junctions. To keep a continuous model, we decrease the size of the junction without neglecting the current crossing it. Then  $g$  tends to a sum of delta functions<sup>22,23</sup>:

$$\begin{aligned} \nabla^2 \psi + \sum_{j=1}^N d_j \delta(x - a_j) \sin \psi &= 0; \quad d_j = \frac{w_j l_j}{w/2}; \\ \psi|_{y=0} &= H = \frac{1}{2w} I; \end{aligned} \quad (3)$$

Despite its theoretical aspect, the delta function allows a detailed mathematical analysis of the solutions<sup>23</sup>.

As opposed to standard models of this type of device<sup>1,2,6</sup>, our approach does not neglect the variation of  $\psi$  in the linear part of the circuit. This allows, for example, to show the differences between inline and overlap current feed. The main advantage of eq.(3) is that we can choose the position  $a_j$  and size ( $w_j; l_j$ ) of each junction and that we satisfy the matching conditions that exist in the original problem (2). We have shown<sup>23</sup> the periodicity of  $\psi_{\text{max}}$  curve for an array where the junction positions are rational and analyzed the differences between inline and overlap current feed, the effect of one remote junction on the array etc... There we established that for a device with sufficiently small junctions, the  $\psi_{\text{max}}$  curve of eq.(3) tends to a simple function called the magnetic approximation.

For the device A (resp. B) (see Table 1),  $d_j = 0.025$ . (resp.  $d_j = 0.0178$  ::). For such small coefficients, the magnetic current which flows the junctions does not affect much the phase in the linear parts of eq.(3). In this case, the phase gradient is proportional to the magnetic field  $H$  (see eq.(3)). We therefore assume that  $\psi(x) = Hx + c$ , so  $\psi = \sum_j d_j \sin(Ha_j + c)$ .

To find the  $\psi_{\text{max}}(H)$  curve for the magnetic approximation, we take the derivative of  $\psi$  with respect to  $c$ . The values of  $c$  such that  $\partial \psi / \partial c = 0$  are

$$G_{\text{max}}(H) = \arctan \frac{\sum_{j=1}^N d_j \cos(Ha_j)}{\sum_{j=1}^N d_j \sin(Ha_j)}, \text{ we obtain}$$

$$\psi_{\text{max}}(H) = \sum_{j=1}^N d_j \sin(Ha_j + G_{\text{max}}(H)) : \quad (4)$$

The absolute value is to guarantee that this is a maximum and not an extremum. This generalizes the stan-

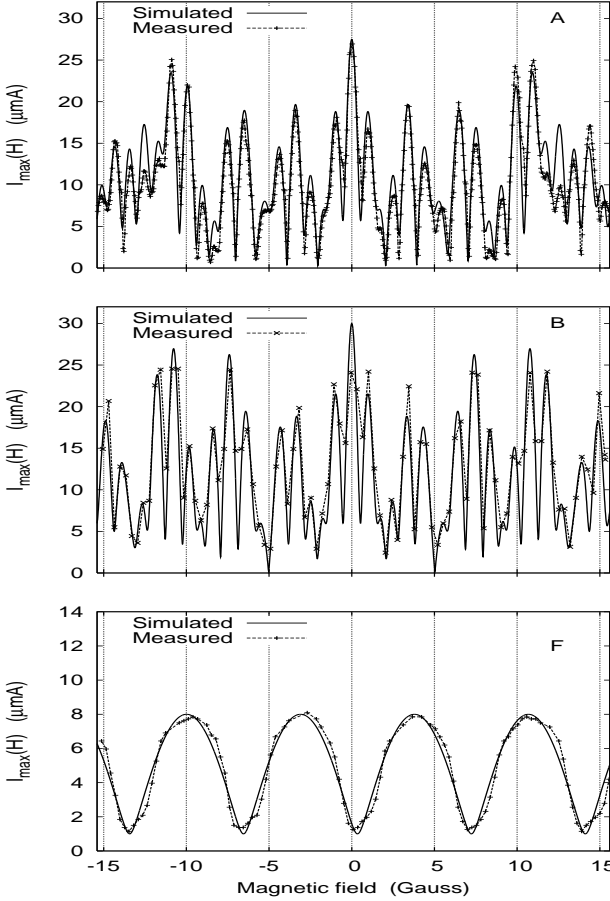


FIG. 2: Measured and simulated (see eq.(4))  $I_{m,ax}(H)$  in the  $V = 0$  state versus  $H$  at 4.2K for the arrays of junctions: A, B and F. Notice that for the device F, we simulate the device with one junction with an area  $1.1 \text{ m}^2$  and the second  $0.9 \text{ m}^2$ .

standard approach<sup>2,6</sup>. Fig.2 shows the measured and simulated supercurrent  $I_{m,ax}(H)$  for the circuits A, B and C, with the  $H$  field applied along the y-axis. All circuits are from the same batch and F was used to calibrate the measurements and validate the numerical model. As an additional test of the model, we computed  $I_{m,ax}(H)$  curves of arrays with  $N = 5, 10$  and  $20$  periodically spaced junctions, and obtained the same patterns reported in other works<sup>8</sup>. The experimental  $I_{m,ax}(H)$  curves were all measured at 4.2K. The magnetic field was produced by a superconducting electromagnet calibrated with a cryogenic Hall probe. Fig.2 is a blow-up of the region near  $H = 0$  where the features of the array geometry become visible. On a larger  $H$  scale (300 Gauss corresponds to  $\phi_0$  in a  $1 \text{ m}^2$  junction) all curves follow the well-known Fraunhofer diffraction pattern given by the length  $l_j$  of the junctions. Within this envelope, the  $I_{m,ax}(H)$  curves of A and B follow complex yet reproducible patterns which are geometry-dependent, yet qualitatively similar. The  $I_{m,ax}(H)$  curves of A and B are undisputedly different, showing the extreme sensitiv-

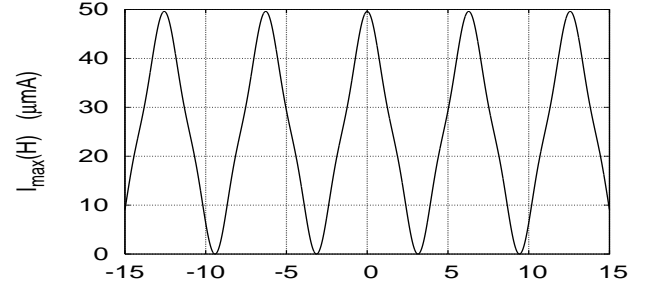


FIG. 3: Simulated  $I_{m,ax}(H)$  curve for an array of 5 junctions such (all lengths are given in  $\mu\text{m}$ )  $w = 5$ ,  $a_1 = 2$ ,  $l_1 = 21.2$ ,  $l_2 = 10.6$ ,  $l_3 = 10.6$ ,  $l_4 = 21.2$  and respective area of the junction are (given in  $\text{m}^2$ ):  $0.24, 2.24, 4.96, 2.24, 0.24$  and  $J_c = 5 \text{ kA cm}^{-2}$ .

ity of the Josephson "interference" to junction distribution. In Figs 2A and B, the measured  $I_{m,ax}(H)$  curves were smaller than expected from  $I_c$ . This can be due to the difference in magnetic thicknesses  $d$  in the junction and microstrip that we neglect<sup>20</sup>. The simulated curves of A, B and F are homothetically adjusted on the current axis by respectively the factors 260, 270 and 201. For the  $H$  axis, the needed adjustment factors are 0.8, 0.8 and 1 and in the case of F an offset of 2.8 Gauss is compensated for. For the SQUID (F) we had to slightly correct the area of one of the junctions to fit  $I_{m,ax}(H)$  and get its smooth behavior near the minimum instead of the sharp behavior obtained for identical junctions<sup>23</sup>. The periodicity of  $I_{m,ax}(H)$  in the SQUID is  $H_0 = 4.8$  Gauss, close to the theoretical value  $H_0 = 4.6$  Gauss, derived from a calculated effective magnetic permeability  $1.68$  in the  $NbSiO/Nb$  stripline. The ratio of the bumps average widths in the  $N = 5$  and  $N = 2$  cases is  $8$ , which is the ratio of the circuits lengths. For  $l = 80 \text{ m}$ ,  $H = 0.6$  Gauss corresponds to  $\phi_0$ . The narrow ( $0.5 - 0.8$  Gauss) bumps for the  $N = 5$  arrays therefore correspond to supercurrent vortices extending over the whole circuit, indicating that the phase distributes itself over the whole device.

Most experimental and numerical studies of vortices in DJTLs have dealt with uniform arrays<sup>4,16,17,24</sup> and large junction numbers ( $N > 10$ ). In such a DJTLs with  $j < 1$ , vortices experience pinning and therefore the "nuls" in  $I_{m,ax}(H)$  do not reach  $I = 0$  but a  $I_{m,in} \neq 0$  floor which rises with  $j^{1/7}$ . The non-uniform arrays reported here have different non-zero  $I_{m,in}$  values for all minima and since all bumps in  $I_{m,ax}(H)$  are clearly seen, vortex pinning is moderate. We expect mobile vortices in the circuit A because  $j = 1.78 > 1$  ( $J_c = 5 \text{ kA cm}^{-2}$ ). We observed<sup>13</sup> several constant-voltage branches in the IVCs of A, B and other non-uniform arrays, due to Josephson resonances. Their frequencies  $f_n$  and their shapes suggest traveling vortices. We have also seen such branches in the numerical solutions for given voltages.

Fluxon propagation in LJJs has been extensively studied for submillimeter-wave flux-ow oscillations.

tors (FFOs) in superconducting integrated heterodyne receivers<sup>3,9</sup>. Non-uniform DJTLs hosting vortices offer advantages over LJJ's for FFOs<sup>14</sup>. Whereas broadband rf coupling is a challenge for the very-low impedance LJJ's, non-uniform DJTLs such as discussed in this Letter were optimally designed for this. Also, tunneling and stripline regions distinct in a DJTL allow to adjust separately quasiparticle loss and surface loss parameters which jointly determine the oscillator mode (resonant vs. flux-ow)<sup>8</sup>. Such non-uniform DJTLs could also be useful in vortex-based electronics.

Our mathematical model, validated by measures, allows to develop non-uniform DJTLs for magnetometry (SQIFs). It can also be used to improve their performance as Josephson magnetic filters. For instance, microwave circuits and sensors using quasiparticles should be most insensitive to H noise. To reduce Josephson noise in SIS mixers one biases them with a magnet on the

zeroes of their  $I_{m,ax}(H)$  curve. But mixer stability is limited by how narrow the dips are at one zero. A specially designed non-uniform SIS array with zeroes considerably attenuated and set at specified H values would solve this problem. Just as an active antenna array can synthesize a given microwave beam shape, non-uniform DJTLs can produce a given  $I_{m,ax}(H)$  curve and our model can be reversely applied to derive the required geometry. As an example, Fig.3 shows the simulated triangular-periodic  $I_{m,ax}(H)$  pattern corresponding to a  $N = 5$  array with various junction spacings and sizes. This geometry can be realized by optical lithography. Other patterns where  $I_{m,ax}(H)$  is zero on an interval can also be generated.

While at LERMA, M.-H. Chung of Taeduk Observatory developed the code for SIS mixing in DJTLs. We acknowledge Y. Delorme, F. Dauplay, B. Lecomte, A. Feret and J.-M. Krieger for their contribution to the SIS mixer work.

- <sup>1</sup> A. Barone and G. Paterno, *Physics and Applications of the Josephson effect*, Wiley, (1982).
- <sup>2</sup> K. Likharev, *Dynamics of Josephson junctions and circuits*, Gordon and Breach, (1986).
- <sup>3</sup> A. V. Ustinov, *Physica D* 123, 315 (1998).
- <sup>4</sup> M. Peyrard and M. D. Kruksal, *Physica D* 14, 88 (1984).
- <sup>5</sup> K. Nakajima, H. Mizusawa, Y. Sawada, H. Akoh and S. Takada, *Phys. Rev. Lett.* 65, 1667 (1990).
- <sup>6</sup> J. H. Miller, Jr., G. H. Gunaratne, J. Huang, and T. D. Golding, *Appl. Phys. Lett.* 59, (25), 3330 (1991).
- <sup>7</sup> H. S. J. van der Zant, D. Berman, T. P. Orlando, and K. A. Delin, *Phys. Rev. B* 49, (18), 12945 (1994).
- <sup>8</sup> V. P. Koshelets and S. V. Shitov, *Supercond. Sci. Technol.* 13, R53-R69 (2000).
- <sup>9</sup> J. Oppenlander, Ch. Haussler, and N. Schopohl, *Phys. Rev. B* 63, 24511p. 4511 (2001).
- <sup>10</sup> J. Zmuidzinas and P. L. Richards, *Proc. IEEE* 92, 10, p.1597 (2004)
- <sup>11</sup> M. Salez et al., *Proc. SPIE Conf. on Telescopes and Astronomical Instrumentation*, Hawaii, 2002 (August 22-28), vol. 4855, p. 402.
- <sup>12</sup> S. C. Shi, T. Noguchi, J. Inatani, Y. Irimajiri, and T. Saito, *IEEE Microwave and Guided Wave Lett.* 8, 11, (1998).
- <sup>13</sup> M. Salez et al., *Proc. 11<sup>th</sup> Intern. Symp. Space THz Techn.*, Ann Arbor, 2000 (May 1-3), p. 343.
- <sup>14</sup> M. Takeda and T. Noguchi, *IEEE Trans. Microwave Theory and Techn.* 50, p. 2618 (2002)
- <sup>15</sup> A. V. Ustinov, M. Cirillo, B. H. Larsen, V. A. Obzovov, P. Carelli, and G. Rotoli, *Phys. Rev. B* 51, (5), 3081 (1995).
- <sup>16</sup> H. S. J. van der Zant, T. P. Orlando, S. Watanabe, and S. H. Strogatz, *Phys. Rev. Lett.* 74, 174 (1995).
- <sup>17</sup> A. E. Duwel, S. Watanabe, E. Trias, T. P. Orlando, H. S. J. van der Zant, and S. H. Strogatz, *J. Appl. Phys.* 82, 4661 (1997).
- <sup>18</sup> J. G. Caputo, N. Flytzanis, Y. Gaididei and M. Valvanis, *ev. E* 54, N2, 2092-2101 (1996).
- <sup>19</sup> M. H. Chung and M. Salez, *Proc. 4th European Conference on applied superconductivity, EUCA S 99*, 651, (1999).
- <sup>20</sup> J. G. Caputo, N. Flytzanis and M. Vavalis, *International Journal of Modern Physics C*, vol. 6, No. 2, 241-262, (1995); *International Journal of Modern Physics C*, vol. 7, No. 2, 191-216, (1996).
- <sup>21</sup> J. G. Caputo and Y. Gaididei, *Physica C*, 402, 160-173, (2004).
- <sup>22</sup> J. G. Caputo and L. Loukitch, *Physica C* 425 (2005) 69-89.
- <sup>23</sup> J. G. Caputo and L. Loukitch, <http://www.arxiv.org/abs/math-ph/0607018>
- <sup>24</sup> C. E. Tong, R. B. Lundell, B. Bumble, J. A. Stern and H. D. LeDuc, *Appl. Phys. Lett.* 67, 9, 1304, (1995); V. Y. Belitzky and E. L. Kollberg, *J. Appl. Phys.* 80, 4741, (1996).
- <sup>25</sup> F. Boussaha, M. Salez, Y. Delorme, A. Feret, B. Lecomte, K. W. Esterberg, M. Chaubet, *Proc. SPIE, 1st Int. Symp. "Microtechnologies for the New Millennium 2003"*.
- <sup>26</sup> The magnetic depth in a Josephson transmission line is given by  $d = \lambda_e t_d$  where  $\lambda_e = 1 + (\lambda_L = t_d) [\coth(t_d = \lambda_L) + \coth(t_d = \lambda_L)]$  where  $\lambda_L$  is the London depth in niobium and  $t_d, t_1$  and  $t_2$  are respectively the thicknesses of the dielectric layer (junction's tunnel barrier or stripline dielectric) and of the lower and upper electrodes.
- <sup>27</sup> Superconducting parallel arrays of tunnel junctions bear various names in the literature: "discrete Josephson transmission line" (DJTL) in the Josephson physics community<sup>3</sup>, "parallel-connected tunnel junction" (PCTJ) among SIS mixer engineers<sup>12</sup>, "superconducting quantum interference grating" (SQUIGs)<sup>6</sup> or "superconducting quantum interference filters" (SQIFs)<sup>9</sup> in magnetometry. In the limit  $\lambda \rightarrow 0$ , "long Josephson junction" (LJJ) and "distributed quasiparticle SIS mixer"<sup>24</sup> also describe the same object from different perspectives.